INTERFACE

rsif.royalsocietypublishing.org

Report

Cite this article: Antonacci G, Pedrigi RM, Kondiboyina A, Mehta VV, de Silva R, Paterson C, Krams R, Török P. 2015 Quantification of plaque stiffness by Brillouin microscopy in experimental thin cap fibroatheroma. *J. R. Soc. Interface* **12**: 20150843.
http://dx.doi.org/10.1098/rsif.2015.0843

Received: 24 September 2015
Accepted: 22 October 2015

Subject Areas:
biomechanics, biophysics, bioengineering

Keywords:
atherosclerosis, biomechanics, plaque rupture

Author for correspondence:
Peter Török
e-mail: peter.torok@imperial.ac.uk

†These authors contributed equally to the study.

Electronic supplementary material is available at http://dx.doi.org/10.1098/rsif.2015.0843 or via http://rsif.royalsocietypublishing.org.

THE ROYAL SOCIETY PUBLISHING

Quantification of plaque stiffness by Brillouin microscopy in experimental thin cap fibroatheroma

Giuseppe Antonacci[1,4,†], Ryan M. Pedrigi[2,†], Avinash Kondiboyina[2], Vikram V. Mehta[2], Ranil de Silva[3], Carl Paterson[1], Rob Krams[2] and Peter Török[1]

[1]Department of Physics, [2]Department of Bioengineering and [3]National Heart and Lung Institute, Imperial College London, London, UK
[4]Center for Life Nano Science, Istituto Italiano di Tecnologia, Rome, Italy

Plaques vulnerable to rupture are characterized by a thin and stiff fibrous cap overlaying a soft lipid-rich necrotic core. The ability to measure local plaque stiffness directly to quantify plaque stress and predict rupture potential would be very attractive, but no current technology does so. This study seeks to validate the use of Brillouin microscopy to measure the Brillouin frequency shift, which is related to stiffness, within vulnerable plaques. The left carotid artery of an ApoE$^{-/-}$ mouse was instrumented with a cuff that induced vulnerable plaque development in nine weeks. Adjacent histological sections from the instrumented and control arteries were stained for either lipids or collagen content, or imaged with confocal Brillouin microscopy. Mean Brillouin frequency shift was 15.79 ± 0.09 GHz in the plaque compared with 16.24 ± 0.15 ($p < 0.002$) and 17.16 ± 0.56 GHz ($p < 0.002$) in the media of the diseased and control vessel sections, respectively. In addition, frequency shift exhibited a strong inverse correlation with lipid area of -0.67 ± 0.06 ($p < 0.01$) and strong direct correlation with collagen area of 0.71 ± 0.15 ($p < 0.05$). This is the first study, to the best of our knowledge, to apply Brillouin spectroscopy to quantify atherosclerotic plaque stiffness, which motivates combining this technology with intravascular imaging to improve detection of vulnerable plaques in patients.

1. Introduction

Acute coronary syndrome is a leading cause of death in coronary heart disease, which results from rupture of an atherosclerotic plaque causing thrombosis, coronary occlusion and myocardial infarction [1]. Plaques vulnerable to rupture are characterized by a large plaque burden with a large, lipid-rich necrotic core covered by a thin and inflamed fibrous cap that is less than 65 μm thick. These plaques are called thin cap fibroatheromas (TCFAs) [2].

It is widely regarded that the process of acute TCFA rupture is principally a mechanical phenomenon, caused by stress concentrations occurring at the interface of the stiff fibrous cap and the compliant (non-load-bearing) necrotic core [3]. The principal factor limiting *in vivo* characterization of plaque stress concentrations is the inability to quantify patient-specific plaque stiffness locally [4]. Thus, there is a strong rationale to develop a new imaging modality that enables direct measurement of plaque stiffness at high-resolution *in vivo*. Such a technology would enhance the ability to accurately compute plaque stress concentrations and improve identification of TCFA at risk of catastrophic rupture.

Confocal Brillouin microscopy is an optical, non-contact method to image three-dimensional spatial variations in the frequency of the Brillouin-scattered light across a sample [5]. The spectrum of light scattered by thermal acoustic waves in the sample is analysed to measure the Brillouin frequency shift, which is related to the elastic modulus (see electronic supplementary material for further details). Brillouin microscopy has been used to measure the

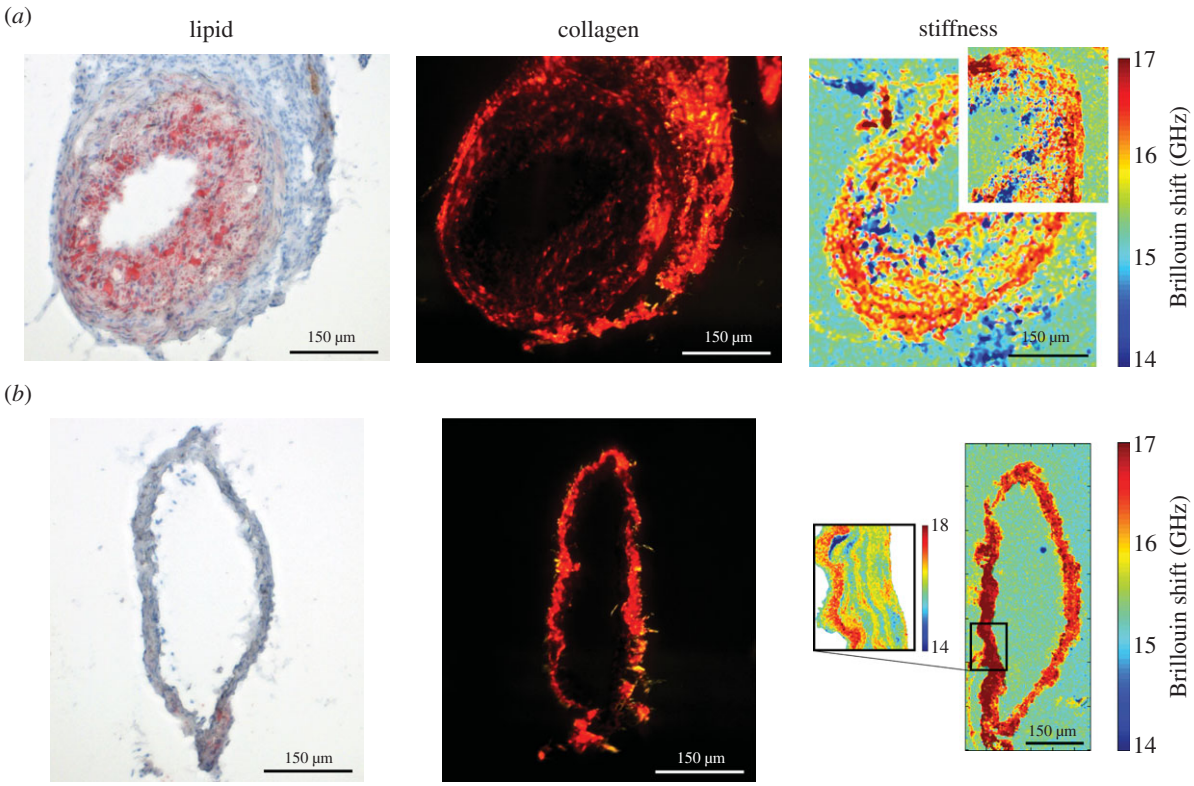

Figure 1. Images of (left) lipid (imaged with light microscopy), (centre) collagen (imaged with polarized light microscopy) and (right) Brillouin shift (imaged with Brillouin microscopy), which is related to stiffness, obtained from representative neighbouring sections of the (*a*) instrumented and (*b*) control vessels**.** In each Brillouin image, a small region was selected to perform a higher resolution scan to demonstrate the power of the technique. The instrumented vessel section shows a fully developed TCFA with reduced stiffness in the intimal region, which is expected due to the soft necrotic core of the plaque. In contrast, the control section has no visible plaque and more constant, higher values of stiffness. Owing to shrinkage associated with the fixation process, histology sections are smaller than unfixed Brillouin sections, which is an artefact that is accounted for in the co-registration process. Scale bars, 150 μm. (Online version in colour.)

frequency shift of the eye lens [6] and cornea [7], including a human lens *in vivo* [8], and it has been recently shown to be capable of subcellular resolution [9]. Herein, we designed and built a high-resolution confocal Brillouin microscope and used it to measure local frequency shift variations of mouse carotid artery sections containing TCFA.

2. Methods

2.1. Brillouin microscopy system

A confocal Brillouin microscope was designed to acquire two-dimensional high spatial resolution images of Brillouin frequency shift, which is related to stiffness (see electronic supplementary material, Methods). Electronic supplementary material, figure S1 shows a diagram of the optical system. A backscattering geometry was used to minimize the spectral broadening of the Brillouin peaks owing to the high numerical aperture (NA) lens used [9]. The light of a single longitudinal-mode laser ($\lambda = 561$ nm) was focused onto the sample by an oil-immersion microscope objective lens (100×, NA = 1.3). The scattered light, collected by the same lens, was spectrally analysed by a 60 dB extinction two-stage spectrometer based on a modified Fabry–Periot etalon (virtually imaged phased array) interferometer [10]. The spectra were captured by a sCMOS camera set to 0.2 s acquisition time. Raster scanning of the sample was performed by a motorized stage of 40 nm minimum step size. At each point of the sample (pixel), the frequency shift of the Brillouin-scattered light was determined by fitting a Lorentzian function on the spectrum. The fitting accuracy of the Lorentzian depends on the number of photons acquired by the camera, but for photon yields typical in Brillouin microscopy, the accuracy is higher than the spectral resolution of our set-up. This approach yielded a Brillouin frequency shift distribution over the entire sample. The aberration-limited resolution of our microscope is 300 nm (transversal) and 1.54 μm (axial).

2.2. Comparing spatial distributions of lipid and stiffness in thin cap fibroatheromas

One ApoE$^{-/-}$mouse was initiated on a high-fat diet and, two weeks later, instrumented with a blood flow-modifying cuff around the left carotid artery that caused the development of TCFA at nine weeks [11]. After culling the animal, both carotid arteries were excised and serially sectioned over the entire TCFA. Alternating sections were imaged with Brillouin microscopy to obtain a frequency shift distribution for each imaged section that was co-registered to both a lipid (oil-red-O) and collagen (picrosirius red) distribution, which were obtained by staining adjacent sections and imaging them with light microscopy ($n = 5$ pairs between shift and each stain, the sections between each pairing of which were a mean of 22.4 ± 14.3 and 30.4 ± 14.3 μm apart for lipid and collagen, respectively). Each pair of co-registered shift–stain distributions was used to investigate how regions containing increasing amounts of soft lipid or stiff collagen correlated to the frequency shift given by Brillouin microscopy. Because paired sections were not identical (only adjacent), values of shift and stain area were circumferentially averaged at 20 radial locations through the section thickness prior to performing the correlation analysis (see electronic supplementary material, Methods for further details).

2.3. Statistics

Data are presented as mean ± s.d. Statistical comparisons between the intima and media of diseased and control artery sections were performed with a one-way ANOVA, and a Bonferroni correction was used to account for multiple comparisons by multiplying the *p*-value from the ANOVA by the number of comparisons.

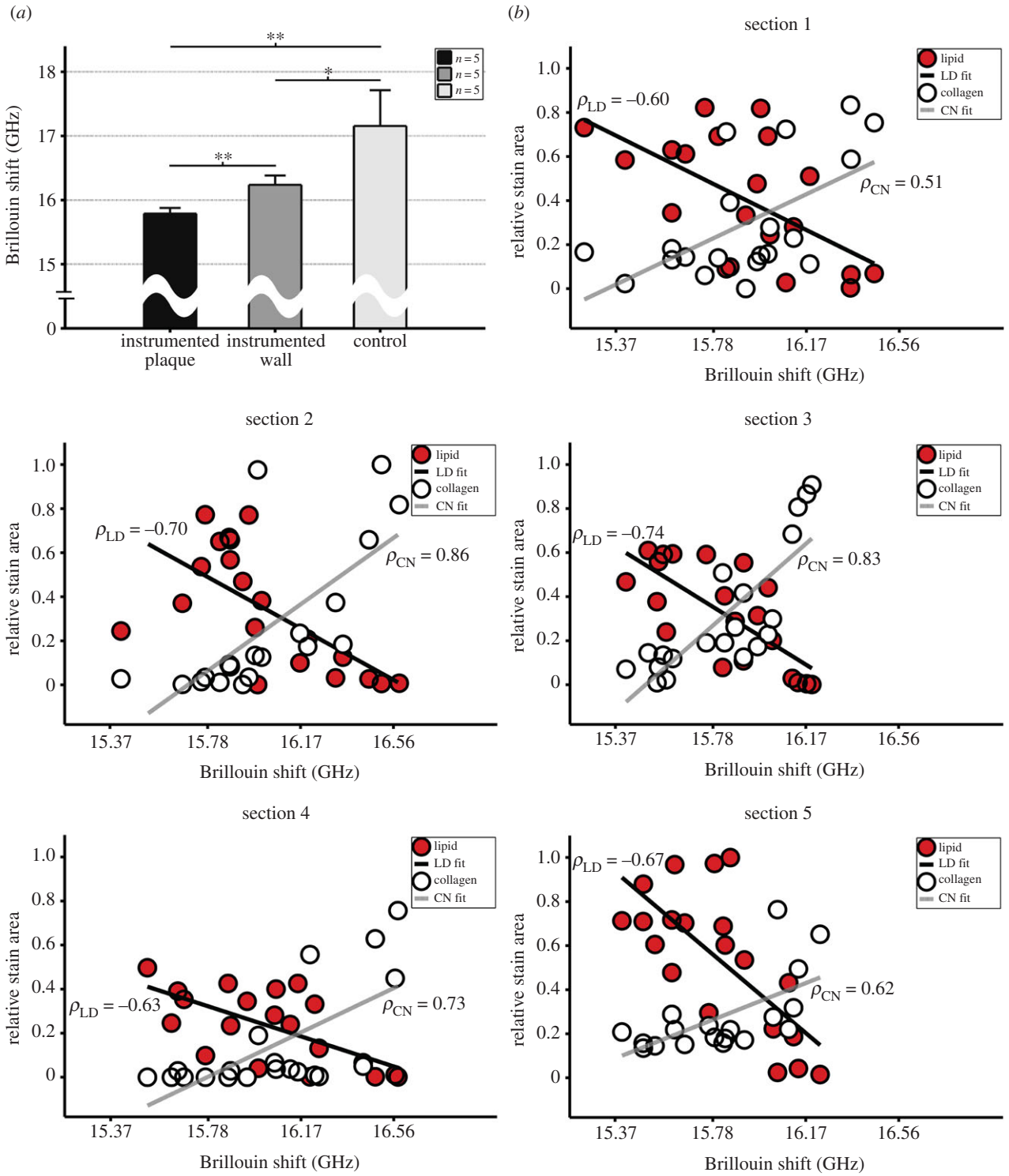

Figure 2. (*a*) The Brillouin shift was reduced within the instrumented vessel intima (region of TCFA) and media, compared with the entire control sections (**$p <$ 0.01 and *$p < 0.05$, respectively; the intima and media of control sections are analysed together because they are not easily distinguished in the absence of plaque). Bars are standard deviation. (*b*) Lipid and collagen stain area (scaled by the maximum of each across all sections to facilitate comparisons) versus Brillouin shift (GHz) for all (20) points of each set of five shift–stain section pairs. Compared with Brillouin shift, lipid showed a strong inverse correlation (mean of -0.67 ± 0.06; $p < 0.01$) and collagen showed a strong direct correlation (0.71 ± 0.15; $p < 0.05$). Black line shows fit from linear regression for lipid (LD) and grey line shows fit for collagen (CN) with the associated Spearman correlation coefficient (ρ). (Online version in colour.)

The threshold for statistical significance was set at $p < 0.05$. The relationship between stain area and Brillouin shift was assessed by computing a Spearman's correlation coefficient. All statistical analyses were performed in Matlab R2012a.

3. Results

TCFA sections exhibited a large plaque burden (computed as the percentage of plaque area to external elastic membrane area [12]) of $60.99 \pm 2.32\%$, averaged over all sections ($n = 5$), with high lipid uptake that was densely distributed across the plaque (figure 1*a*). Correspondingly, the Brillouin shift (a measure of stiffness) distribution was highly variable within individual sections of the diseased vessel (figure 1*a*), although the mean was consistent between sections with values in the plaque regions of 15.79 ± 0.09 compared with 16.24 ± 0.15 GHz within the media of those sections (figure 2*a*; $p < 0.002$). In contrast, the contralateral control sections had no plaque development and

more constant Brillouin shift values over individual sections (figure 1*b*), the mean of which across all sections was 17.16 ± 0.56 GHz. This mean frequency shift of the control sections was significantly higher than that within the plaque ($p < 0.002$) and media ($p < 0.05$) of the TCFA sections (figure 2*a*).

To assess the accuracy of Brillouin microscopy on a local scale, we co-registered the Brillouin shift distributions of each section to both lipid and collagen distributions from neighbouring sections and computed a Spearman's correlation coefficient. There was a strong inverse relationship between Brillouin shift and lipid area for each of the five pairs of co-registered sections, wherein the mean correlation coefficient was -0.67 ± 0.06 ($p < 0.01$; figure 2*b*). In contrast, there was a strong direct correlation between shift and collagen area, the mean of which was 0.71 ± 0.15 ($p < 0.05$; figure 2*b*).

4. Discussion

Brillouin imaging was first reported in 2005 [13] to study the mechanics of ocular tissues at low spatial resolution (NA < 0.2). In this study, we used a high-resolution Brillouin microscope (NA = 1.3) to measure the frequency shift, which is related to tissue stiffness, in atherosclerotic artery sections. To the best of our knowledge, this is the first application of high spatial resolution Brillouin microscopy to evaluate the stiffness of a diseased artery. We demonstrated a strong inverse correlation between Brillouin frequency shift and the local accumulation of lipid, which has a very low stiffness and a heterogeneous distribution within plaques [14]. Conversely, we demonstrated a direct relationship between frequency shift and collagen. Collagen is a primary structural constituent of the normal vessel wall [15] (it is also found in plaques, particularly fibrotic regions like the cap), and it has a stiffness that is much higher than lipid [16]. Collectively, these results validate Brillouin microscopy as a method to optically measure stiffness in atherosclerotic vessel sections.

Ultimately, our work aims to provide tissue elasticity data for rigorous numerical modelling of mechanical stress distributions within the diseased artery wall. Currently, our Brillouin microscopy data cannot be used to accurately quantify the spatial distribution of the elastic modulus in the samples studied. To overcome this limitation, future work will employ quantitative phase imaging within our microscope set-up to determine the average refractive index within the probe volume. This addition, combined with a tissue morphology-based estimation of the material density, will permit an accurate calculation of the local Brillouin modulus and, in turn, a mean elastic modulus.

Accurately computing plaque stress concentrations is considered key to predicting rupture, and it is primarily a function of local vessel stiffness, geometry and blood pressure. Currently, only vessel geometry and blood pressure can be obtained through catheter-based technologies, but not vessel stiffness [3]. Our results show that vessel stiffness can be determined using Brillouin spectroscopy. This finding provides the basis for development of a combined optical coherence tomography–Brillouin spectroscopy catheter system that would enable simultaneous measurement of vessel geometry and stiffness to determine local plaque stress concentrations *in vivo*.

Authors' contributions. G.A., R.M.P., C.P., R.K., and P.T. defined the experimental design. R.M.P., R.d.S. and R.K. interpreted the results. G.A., R.M.P. and V.V.M. performed the experiments. R.M.P. and A.K. analysed the data. All authors contributed to writing the manuscript.

Funding. We thank the BHF for financial support (BHF RG/11/13/29055).

Competing interests. We declare we have no competing interests.

Acknowledgements. Thanks to Ms Lorraine Lawrence for performing the picrosirius red stain and Prof. Steve Greenwald for assistance with polarized imaging of the stain.

References

1. Libby P. 2013 Mechanisms of acute coronary syndromes. *N. Engl. J. Med.* **369**, 883–884. (doi:10.1056/NEJMc1307806)
2. Virmani R, Burke AP, Kolodgie FD, Farb A. 2003 Pathology of the thin-cap fibroatheroma: a type of vulnerable plaque. *J. Interv. Cardiol.* **16**, 267–272. (doi:10.1034/j.1600-0854.2003.8042.x)
3. Pedrigi RM, de Silva R, Bovens SM, Mehta VV, Petretto E, Krams R. 2014 Thin-cap fibroatheroma rupture is associated with a fine interplay of shear and wall stress. *Arterioscler. Thromb. Vasc. Biol.* **34**, 2224–2231. (doi:10.1161/ATVBAHA.114.303426)
4. Holzapfel GA, Mulvihill JJ, Cunnane EM, Walsh MT. 2014 Computational approaches for analyzing the mechanics of atherosclerotic plaques: a review. *J. Biomech.* **47**, 859–869. (doi:10.1016/j.jbiomech.2014.01.011)
5. Scarcelli G, Yun SH. 2007 Confocal Brillouin microscopy for three-dimensional mechanical imaging. *Nat. Photon.* **2**, 39–43. (doi:10.1038/nphoton.2007.250)
6. Scarcelli G, Kim P, Yun SH. 2011 *In vivo* measurement of age-related stiffening in the crystalline lens by Brillouin optical microscopy. *Biophys. J.* **101**, 1539–1545. (doi:10.1016/j.bpj.2011.08.008)
7. Scarcelli G, Kling S, Quijano E, Pineda R, Marcos S, Yun SH. 2013 Brillouin microscopy of collagen crosslinking: noncontact depth-dependent analysis of corneal elastic modulus. *Invest. Ophthalmol. Vis. Sci.* **54**, 1418–1425. (doi:10.1167/iovs.12-11387)
8. Scarcelli G, Yun SH. 2012 *In vivo* Brillouin optical microscopy of the human eye. *Opt. Express.* **20**, 9197–9202. (doi:10.1364/OE.20.009197)
9. Antonacci G, Foreman MR, Paterson C, Torok P. 2013 Spectral broadening in Brillouin imaging. *Appl. Phys. Lett.* **103**, 221105. (doi:10.1063/1.4836477)
10. Scarcelli G, Yun SH. 2011 Multistage VIPA etalons for high-extinction parallel Brillouin spectroscopy. *Opt. Express.* **19**, 10 913–10 922. (doi:10.1364/Oe.19.010913)
11. Cheng C, Tempel D, van Haperen R, van der Baan A, Grosveld F, Daemen MJ, Krams R, de Crom R. 2006 Atherosclerotic lesion size and vulnerability are determined by patterns of fluid shear stress. *Circulation* **113**, 2744–2753. (doi:10.1161/CIRCULATIONAHA.105.590018)
12. Samady H, Eshtehardi P, McDaniel MC, Suo J, Dhawan SS, Maynard C, Timmins LH, Quyyumi AA, Giddens DP. 2011 Coronary artery wall shear stress is associated with progression and transformation of atherosclerotic plaque and arterial remodeling in patients with coronary artery disease. *Circulation* **124**, 779–788. (doi:10.1161/CIRCULATIONAHA.111.021824)
13. Koski KJ, Yarger JL. 2005 Brillouin imaging. *Appl. Phys. Lett.* **87**, 061903. (doi:10.1063/1.1999857)
14. Tracqui P, Broisat A, Toczek J, Mesnier N, Ohayon J, Riou L. 2011 Mapping elasticity moduli of atherosclerotic plaque *in situ* via atomic force microscopy. *J. Struct. Biol.* **174**, 115–123. (doi:10.1016/j.jsb.2011.01.010)
15. Valentin A, Humphrey JD, Holzapfel GA. 2013 A finite element-based constrained mixture implementation for arterial growth, remodeling, and adaptation: theory and numerical verification. *Int. J. Numer. Methods Biomed. Eng.* **29**, 822–849. (doi:10.1002/cnm.2555)
16. Holzapfel GA, Sommer G, Regitnig P. 2004 Anisotropic mechanical properties of tissue components in human atherosclerotic plaques. *J. Biomech. Eng.* **126**, 657–665. (doi:10.1115/1.1800557)